

**SYNTHESIS AND CHARACTERIZATION OF
Fe_xO_y DOPED TiO₂ IMMOBILIZED ON
ACTIVATED CARBON FOR DEGRADATION OF
SINGLE AND BINARY MIXTURE OF
METHYLENE BLUE AND METHYL ORANGE
DYES UNDER VISIBLE LIGHT**

NURUL FITRAHANIS BINTI RAZALI

**UNIVERSITI SAINS MALAYSIA
2018**

**SYNTHESIS AND CHARACTERIZATION OF
Fe_xO_y DOPED TiO₂ IMMOBILIZED ON
ACTIVATED CARBON FOR DEGRADATION OF
SINGLE AND BINARY MIXTURE OF
METHYLENE BLUE AND METHYL ORANGE
DYES UNDER VISIBLE LIGHT**

by

NURUL FITRAHANIS BINTI RAZALI

Thesis submitted in fulfillment of the requirement

for the degree of

Master of Sciences

August 2018

ACKNOWLEDGEMENT

First of all thanks to ALLAH S.W.T, the most beneficent and the most merciful, for guiding me to the right path and keeping me strong to finish this thesis. My sincere thanks to my supervisor Professor Dr Rohana Binti Adnan for giving me the opportunity to work on such a fascinating project with the continuous guidance and supports throughout my study.

Many thanks to my co-supervisor Dr Sumiyyah Sabar for her guidance and suggestions to improve my research skills. Special thanks to my colleagues, Shikin Faezah Binti Soib, Nur Farah Binti Waheed Tajuddin, Nurul Syamimi Binti Abdul Satar, Azia Wahida Binti Aziz, Dr Najm Us Saqib, Dr Irfan Shah, and Jaga for their helps, valuable supports and advices. I would like to acknowledge Universiti Sains Malaysia for RUI grant (1001/PKIMIA/811333) for the financial supports.

Finally, I must express my profound gratitude to my parents, Razali Bin Mohd Desa and Rohana Binti Harun for their countless support because this accomplishment would not have been possible without them. May Allah grant highest place in jannah for both of them. Then, thanks to my siblings and to my best friend Nik Nornadia Binti Nik Leh for providing me unfailing support and continuous encouragement throughout my study.

May Allah bless and grant happiness to those who have supported me along the way to complete this study.

TABLE OF CONTENTS

ACKNOWLEDGEMENT	ii
TABLE OF CONTENTS	iii
LIST OF TABLES	vii
LIST OF FIGURES	ix
LIST OF ABBREVIATIONS	xii
ABSTRAK	xiv
ABSTRACT	xvi
CHAPTER 1: INTRODUCTION	1
1.1 Background	1
1.2 Various types of pollutants in water	1
1.3 Principles of photocatalysis	2
1.4 Titanium dioxide	3
1.4.1 Properties of titanium dioxide	3
1.4.2 Mechanism of photocatalysis using TiO ₂ nanoparticles	5
1.5 Synthesis methods of TiO ₂ nanoparticles	7
1.5.1 Sol-gel	7
1.5.2 Hydrothermal	8
1.5.3 Templating	9
1.5.4 Chemical vapor deposition (CVD).....	10
1.6 Limitations of TiO ₂ nanoparticles	10
1.7 Modification of TiO ₂	11
1.7.1 Doping with metal.....	11
1.7.2 Doping with non-metal	12

1.7.3 Hybrid nanomaterials	13
1.7.4 Dye sensitization of TiO ₂	15
1.7.5 Modification of TiO ₂ by inorganic adsorbates.....	16
1.8 Immobilization of TiO ₂ nanoparticles.....	16
1.9 Regeneration of TiO ₂ nanoparticles	18
1.10 Methylene blue and Methyl orange as model pollutants	20
1.11 Problem statements	24
1.12 Research objectives.....	24
1.13 Scope of study	25
CHAPTER 2: MATERIALS AND METHODS	26
2.1 List of chemicals	26
2.2 Preparation of TiO ₂ and modified TiO ₂ nanoparticles.....	27
2.3 Preparation of TiO ₂ nanoparticles immobilized onto AC.....	27
2.4 Preparation of Fe _x O _y doped nanoparticles immobilized on AC.....	27
2.5 Point of zero charge (pHpzc) studies	27
2.6 Photocatalytic activity studies.....	29
2.6.1 Effect of dye initial concentrations	29
2.6.2 Effect of catalyst dosage	30
2.6.3 Effect of pH	30
2.6.4 Kinetic studies.....	31
2.6.5 Equilibrium adsorption isotherms.....	31
2.7 Regeneration of TiO ₂ nanoparticles	32
2.8 Characterization of TiO ₂ and Fe _x O _y modified TiO ₂	32

CHAPTER 3: RESULTS AND DISCUSSION	35
3.1 Characterization of the TiO ₂ nanoparticles	35
3.1.1 XRD analysis	35
3.1.2 Electron microscopy analysis.....	39
3.1.3 N ₂ adsorption-desorption isotherm analysis of TiO ₂	43
3.1.4 UV-Vis Diffused Reflectance Spectroscopy analysis.....	45
3.1.5 FTIR spectroscopy	48
3.1.6 TG-DTA analysis	49
3.2 Point of zero charge (pH _{pzc})	52
3.3 Photocatalytic activity studies of single dye	54
3.3.1 Effect of dosage.....	54
3.3.2 Effect of dye initial concentration.....	59
3.3.3 Effect of pH.....	64
3.3.4 Effect of dye removal in dark.....	67
3.3.5 Effect of contact times	70
3.3.6 Equilibrium adsorption isotherm	72
3.3.7 Kinetic studies.....	77
3.4 Photocatalytic studies of binary dye mixture	81
3.4.1 Effect of different concentration ratios of binary dyes	81
3.4.2 Effect of pH towards the removal of dyes in binary mixture.....	84
3.5 Regeneration of the spent catalysts	86
CHAPTER 4: CONCLUSION	90
4.1 Summary	90
4.2 Recommendations for future works	91

REFERENCES 92

APPENDICES

LIST OF CONFERENCE

LIST OF TABLES

	Page
Table 1.1 Some of the recent studies on hybrid TiO ₂ nanomaterials modifications and their effects	14
Table 1.2 Properties of methylene blue and methyl orange (PubChem Compound database)	21
Table 1.3 Summary of the studies on the removal of methylene blue using TiO ₂ in reported literature	22
Table 1.4 Summary of the studies on the removal of methyl orange using TiO ₂ in reported literature	23
Table 2.1 Properties of powdered AC used in this study	26
Table 3.1 The summary of chemical and physical properties of the pristine TiO ₂ and the modified TiO ₂	38
Table 3.2 The removal efficiencies of MB and MO under normal laboratory light by 0.10 g different TiO ₂ materials ([MB] ₀ = 75 mg/L, [MO] ₀ = 50 mg/L)	59
Table 3.3 The removal efficiency at different MB initial concentration by different TiO ₂	61
Table 3.4 The MO removal efficiency at different initial concentration by different catalyst	63
Table 3.5 The Langmuir and Freundlich parameters and linear regression of MB by different TiO ₂ samples (0.10 g dosage, unadjusted pH = 6.91, [MB] ₀ = 5, 10, 25, 50, 75, 100 mg/L, reaction time: 2 h)	75
Table 3.6 The Langmuir and Freundlich parameters and linear regression of MO by different TiO ₂ samples (0.10 g dosage, unadjusted pH 7.40, [MO] ₀ = 5, 10, 25, 30, 40, 50 mg/L, reaction time: 2 h).	76
Table 3.7 The pseudo- first and pseudo-second order constants and linear regression coefficients of MB (0.10 g dosage, unadjusted pH = 6.91, [MB] ₀ = 75 mg/L)	79

Table 3.8	The pseudo- first and pseudo-second order constants and linear regression coefficients of MO (0.10 g dosage, unadjusted pH 7.40, $[MO]_0 = 50$ mg/L)	80
Table 3.9	Comparison of the removal efficiency of different TiO_2 particles in binary mixture of MB to MO at different ratio concentration (unadjusted pH= 6.55, 0.1 g dosage, 350 rpm shaking speed, 2 h) exposure under normal laboratory light	83

LIST OF FIGURES

		Page
Figure 1.1	Crystalline structures of three different polymorphs of TiO ₂ (a) anatase (b) rutile (c) brookite	4
Figure 1.2	Schematic presentation of the mechanism of TiO ₂ semiconductor mechanism in heterogeneous photocatalysis	7
Figure 1.3	The molecular structures of (a) methylene blue (b) methyl orange	20
Figure 2.1	Flow chart for the preparation of Fe _x O _y doped TiO ₂ immobilized on AC	28
Figure 3.1	XRD diffractograms of (a) TiO ₂ , (b) TiO ₂ -10% AC, (c) 1% Fe _x O _y /TiO ₂ -10% AC, (d) 0.5% Fe _x O _y /TiO ₂ -10% AC, (e) 0.1% Fe _x O _y /TiO ₂ -10% AC nanoparticles calcined at 300 °C for 3 h.	37
Figure 3.2	SEM images and EDX spectra of (a) AC, (b) TiO ₂ , (c) TiO ₂ -10% AC, (d) 1% Fe _x O _y /TiO ₂ -10% AC, (e) 0.5% Fe _x O _y /TiO ₂ -10% AC, (f) 0.1% Fe _x O _y /TiO ₂ -10% AC nanoparticles	40
Figure 3.3	TEM images of (a) AC, (b) TiO ₂ , (c) TiO ₂ -10% AC, (d) 1% Fe _x O _y /TiO ₂ -AC, (e) 0.5% Fe _x O _y /TiO ₂ -10% AC, (f) 0.1% Fe _x O _y /TiO ₂ -10% AC	42
Figure 3.4	N ₂ adsorption-desorption isotherms of (a) TiO ₂ , (b) TiO ₂ -10% AC, (c) 1% Fe _x O _y /TiO ₂ -10% AC, (d) 0.5% Fe _x O _y /TiO ₂ -10% AC, (e) 0.1% Fe _x O _y /TiO ₂ -10% AC nanoparticles	44
Figure 3.5	Direct band gap energy of (a) TiO ₂ , (b) TiO ₂ -10% AC, (c) 1% Fe _x O _y /TiO ₂ -10% AC, (d) 0.5% Fe _x O _y /TiO ₂ -10% AC, (e) 0.1% Fe _x O _y /TiO ₂ -10% AC nanoparticles	46

Figure 3.6	Indirect band gap energy of (a) TiO ₂ , (b) TiO ₂ -10% AC, (c) 1% Fe _x O _y / TiO ₂ -10% AC, (d) 0.5% Fe _x O _y / TiO ₂ -10% AC, (e) 0.1% Fe _x O _y / TiO ₂ -10% AC nanoparticles	47
Figure 3.7	FTIR spectra of TiO ₂ and the modified TiO ₂ after immobilization onto AC and doped with Fe _x O _y	49
Figure 3.8	TG-DTA thermograms of the synthesized TiO ₂ nanoparticles via sol-gel method for (a) TiO ₂ (b) TiO ₂ -10% AC and (c) 0.5% Fe _x O _y /TiO ₂ -10% AC	50
Figure 3.9	pH of point of zero charges of AC, TiO ₂ and the modified TiO ₂ nanoparticles	53
Figure 3.10	Determination of the removal efficiency of MB under normal laboratory light after 2 h by different dosage of TiO ₂ and modified TiO ₂ ([MB] ₀ = 75 mg/L, unadjusted pH = 6.91, shaking speed at 350 rpm)	56
Figure 3.11	Determination of the removal efficiency of MO under normal laboratory light after 2 h by different dosage of TiO ₂ and modified TiO ₂ ([MO] ₀ = 50 mg/L, unadjusted pH = 7.40, shaking speed at 350 rpm)	58
Figure 3.12	Determination of MB removal efficiency under normal laboratory light by different initial concentrations of MB by different TiO ₂ photocatalyst after 2 h (0.10 g dosage, unadjusted pH = 6.91 and shaking speed at 350 rpm)	60
Figure 3.13	Determination of MO removal efficiency under normal laboratory light by different initial concentration of MO by different TiO ₂ after 2 h (0.10 g dosage, unadjusted pH = 7.40, shaking speed at 350 rpm)	62
Figure 3.14	MB removal efficiency under normal laboratory light at different pH by different TiO ₂ after 2 h ([MB] ₀ = 75 mg/L, 0.10 g dosage, unadjusted pH = 6.91, shaking speed at 350 rpm)	65
Figure 3.15	MO removal efficiency under normal laboratory light at different pH by different TiO ₂ photocatalysts after 2 h ([MO] ₀ = 50 mg/L, 0.10 g dosage, shaking speed at 350 rpm)	67
Figure 3.16	Determination of (a) [MB] ₀ = 75 mg/L, unadjusted pH = 6.9, (b) [MO] ₀ = 50 mg/L, unadjusted pH = 7.40, by 0.10	68

g dosage with shaking speed at 350 rpm for the removal efficiency in the dark and under normal laboratory light by different TiO₂

Figure 3.17	Effect of contact time on the removal of MB under normal laboratory light ([MB] _o = 75 mg/L, 0.10 g dosage, unadjusted pH (pH = 6.91), shaking speed at 350 rpm)	71
Figure 3.18	Effect of contact time on the removal of MO at different contact time ([MO] _o = 50 mg/L, 0.10 g dosage, unadjusted pH, pH 7.40, shaking speed at 350 rpm)	72
Figure 3.19	Determination of MB removal at different pH for a mixture containing MB to MO (mg/L) ratio of 40:40 after 2 h exposure under normal laboratory light by different TiO ₂ nanoparticles (0.10 g dosage, shaking speed at 350 rpm)	85
Figure 3.20	Determination of MO removal at different pH of binary solution containing MB to MO (mg/L) ratio of 40:40 after 2 h exposure under normal laboratory light by different TiO ₂ nanoparticles (0.10 g dosage, shaking speed at 350 rpm)	86
Figure 3.21	Regeneration studies of TiO ₂ , and modified TiO ₂ by using different desorbing agents (a) distilled water (b) NaNO ₃ (c) H ₂ SO ₄ (d) NaOH for MB removal ([MB] _o = 75 mg/L, 0.10 g dosage, unadjusted pH (pH = 6.91), shaking speed at 350 rpm)	88
Figure 3.22	Regeneration studies of TiO ₂ , and modified TiO ₂ by using different desorbing agent, (a) distilled water (b) NaNO ₃ (c) H ₂ SO ₄ (d) NaOH for MO removal ([MO] _o = 50 mg/L, 0.10 g dosage, unadjusted pH, pH 7.40, shaking speed at 350 rpm)	89

LIST OF ABBREVIATIONS

AC	Activated Carbon
Ag-GO	Silver Graphene Oxide
AOP	Advanced Oxidation Process
BET	Braunauer Emmett Teller
CB	Conduction Band
CE	Carbon Electrode
CNT	Carbon Nanotube
4-CP	4-chlorophenol
CVD	Chemical Vapor Deposition
DBD	Dielectric Barrier Discharge
DSSC	Dye Sensitized Solar Cells
DTA	Differential Thermal Analysis
DRS	Diffuse Reflectance Spectroscopy
EDX	Energy Dispersion X-ray
e^-	electron
E_g	Band gap energy
FESEM	Field Emission Scanning Electron Microscopy
FTIR	Fourier Transform Infrared Spectroscopy
GAC	Granular Activated Carbon
GF	Graphene Film
GO	Graphene Oxide
h^+	hole
JCPDS	Joint Committee on Powder Diffraction Standards

k	Pseudo-first order rate constant
LECA	Light Expanded Clay Aggregate
MB	Methylene Blue
MO	Methyl Orange
MWCNT	Multiwalled Carbon Nanotubes
NTA	Nano-tube Array
PANI	Polyaniline
pH _{pzc}	pH of Point of Zero Charge
PoPD	poly-o-phenylenediamine
PVA	Polyvinyl Alcohol
R ²	Linear Regression Coefficient
SEM	Scanning Electron Microscopy
sccm	standard cubic centimeter per minute
TEM	Transmission Electron Microscopy
TG/DTA	Thermo Gravimetric/ Differential Thermal Analysis
TTIP	Titanium (IV) tetraisopropoxide
UV	Ultraviolet
VB	Valence band
XRD	X-ray Diffraction

**SINTESIS DAN PENCIRIAN TiO₂ TERDOP Fe_xO_y TERPEGUN KARBON
TERAKTIF UNTUK DEGRADASI PEWARNA TUNGGAL DAN
CAMPURAN BINARI METILENA BIRU DAN METIL OREN DI BAWAH
CAHAYA NAMPAK**

ABSTRAK

Tujuan kajian ini adalah untuk menghasilkan fotomangkin yang mempunyai aktiviti fotomangkinan yang baik di bawah cahaya nampak. Dalam kajian ini pengubahsuaian TiO₂ dilakukan dengan pemegunan ke atas 10 wt % karbon teraktif (TiO₂-10% AC) dan pendopan Fe_xO_y ke atas TiO₂-10% AC dengan peratusan berat Fe yang berbeza (0.1, 0.5, 1% wt) di atas TiO₂-10%AC telah dijalankan menggunakan kaedah sol-gel. Kesan pendopan Fe_xO_y dan pemegunan di atas AC terhadap keupayaan penyingkiran pewarna tunggal, metilena biru (MB) dan metil oren (MO), dan pewarna campuran binari MB dan MO telah dibandingkan dengan TiO₂ tulen. Analisis pembelauan sinar X (XRD) telah menunjukkan bahawa saiz kristal TiO₂ berkurangan daripada 56.5 kepada 24.4 nm selepas pemegunan di atas AC, sementara luas permukaan meningkat daripada 114 kepada 204 m² g⁻¹ dengan peningkatan % wt dopan. Malah, luang jalur fasa anatas TiO₂ juga telah berkurangan daripada 3.15 kepada 2.8 eV apabila peratusan berat dopan Fe_xO_y ditingkatkan kepada 1%. Parameter optima bagi penyingkiran pewarna tunggal MB dan MO telah ditentukan sebagai 0.10 g dos mangkin, 75 mg/L MB, 50 mg/L MO, pada pH ambien dengan masa sentuhan 2 jam. Sementara itu, parameter optima untuk pewarna campuran binari adalah pada nisbah kepekatan tinggi (mg/L) MB kepada MO (40:40) dan pH ambien dengan masa sentuhan 2 jam. Fotomangkin 1% Fe_xO_y/TiO₂-10% AC menunjukkan penyingkiran maksima sebanyak 93% bagi pewarna MB dengan kepekatan awal 75 mg/L, sementara fotomangkin 0.1% Fe_xO_y/TiO₂-10% AC

menunjukkan penyingkiran sehingga 96% bagi MO dengan kepekatan awal 50 mg/L selepas 2 jam penyinaran di bawah cahaya lampu makmal biasa. Fotomangkin 0.5% $\text{Fe}_x\text{O}_y/\text{TiO}_2$ -10 AC menunjukkan penyingkiran tertinggi pewarna campuran binari pada nisbah kepekatan awal 40:40 (mg/L) selepas 2 jam penyinaran dengan masing-masing 88 dan 99% MB dan MO, telah disingkirkan. Kajian ini mendedahkan bahawa pemegunan TiO_2 ke atas AC menambah baik aktiviti fotomangkin zarah nano TiO_2 . Untuk meningkatkan kebolehgunaan semula fotomangkin, ejen penyahjerap yang berbeza seperti H_2O , NaNO_3 , H_2SO_4 , dan NaOH , telah digunakan dan didapati NaOH adalah terbaik bagi MB sementara bagi MO keempat-empat ejen penyahjerap tidak menunjukkan aktiviti penyahjerapan yang baik. Keputusan menunjukkan fotomangkin yang dirawat boleh digunakan semula berulang kali. Walau bagaimanapun peratus penyingkiran menurun kepada 40% pada masing-masing kitaran ke-10 dan ke-3 bagi MB dan MO.

**SYNTHESIS AND CHARACTERIZATION OF Fe_xO_y DOPED TiO₂
IMMOBILIZED ON ACTIVATED CARBON FOR DEGRADATION OF
SINGLE AND BINARY MIXTURE OF METHYLENE BLUE AND METHYL
ORANGE DYES UNDER VISIBLE LIGHT**

ABSTRACT

The purpose of this study is to produce the photocatalyst that has good photocatalytic activity under visible light. In this study the modification of TiO₂ was conducted by immobilization of TiO₂ on 10% wt activated carbon (TiO₂-10% AC) and Fe_xO_y doping of different Fe weight percentages (0.1, 0.5, and 1% wt) on the TiO₂-10%AC using a sol-gel method. The effects of Fe_xO_y doping and immobilization onto AC towards the removal efficiency of single dye methylene blue (MB) and methyl orange (MO), and binary dye mixtures of MB and MO were compared to pure TiO₂. The X-ray diffraction (XRD) analysis showed that the crystallite size of TiO₂ decreased from 56.5 to 24.4 nm after immobilization onto AC, while the surface area increased from 114 to 204 m² g⁻¹ as the % wt of the dopant increased. In fact, the band gap of the anatase phase of TiO₂ was also reduced from 3.15 to 2.8 eV as the % wt of Fe_xO_y dopant were increased to 1%. The optimum parameters for the removal of single MB and MO dyes were determined to be 0.10 g of the catalyst dosage, 75 mg/L of MB, 50 mg/L of MO, at ambient pH with the contact time of 2 h. Meanwhile, the parameters for the binary dyes mixture were found to be optimum at a high concentration (mg/L) ratio of MB to MO (40:40) and at ambient pH with the contact time of 2 h. The 1% Fe_xO_y/TiO₂-10% AC photocatalyst showed maximum removal of 93% for the MB dye with initial concentration of 75 mg/L, while the 0.1% Fe_xO_y/TiO₂-10% AC showed up to 96%

removal for MO with the initial concentration of 50 mg/L after 2 h of irradiation under normal laboratory light. The 0.5% Fe_xO_y/TiO₂-10% AC photocatalyst showed the highest removal of binary dye mixture at the initial concentration ratio of 40:40 (mg/L) after 2 h of irradiation where 88 and 99% of MB and MO were removed, respectively. This study revealed that the immobilization of TiO₂ onto AC improved the photocatalytic activity of the material. To increase the reusability of the photocatalyst, different desorbing agents such as H₂O, NaNO₃, H₂SO₄, and NaOH, were used and it was found that NaOH is the best eluent for MB but for MO none of the desorbing agent shows good desorption activity. The results showed that the treated photocatalysts can be repeatedly used although the percentage of removal decreased to 40% at the 10th and 3rd cycles for MB and MO, respectively.

CHAPTER 1: INTRODUCTION

1.1 Background

Water is one of the most vital element on earth as there will be no life on earth if there is no water. Other than utilizing water for drinking and manufacturing of many products, water is also crucial for cooking, agricultural, and recreational purposes. However, nowadays water pollution has become one of the major source of health problems that are gaining concern around the world.

In Malaysia, residential, commercial, and industrial areas are three main sources that cause water pollution. Various wastewater containing chemicals have been discharged into the water bodies. Water pollution causes adverse effects to human and aquatic life, disturbs the balance of life and reduces the bioavailability of potable water [Yang et al., 2015]. Treatment of the polluted water system is essential to reduce the burden on rivers to supply fresh water considering the demand for clean water is growing as the number of the citizens in Malaysia increases.

1.2 Various types of pollutants in water

There are various types of pollutants in water and this include organic compounds such as sythetic pesticides, antibiotics, detergents, paints, and volatile organic compounds. Most of these pollutants are toxic, have high resistant to microbial degradation, and high stability towards chemical reagents, temperature and Ph [Steng et al., 2013]. Inorganic compounds such as inorganic salts, cyanides, metals compounds, sulphates and mineral acids also affect and contaminate the water body because these compounds are not only toxic but they are also non-biodegradable. Even at low concentrations, these compounds are known to be harmful to human and many aquatic ecosystems. For example, arsenic is highly toxic

and and continuous exposure to arsenic can cause lung, bladder, and kidney cancer (Danish et al., 2013).

Textile industries are one of the major industries that discharged effluents containing large amounts of dyes into the water bodies. Dyes are normally retained in water bodies for a long time, thus contaminating the food chain and affecting animals and human health (Chakravarty et al., 2015).

1.3 Principles of photocatalysis

Photocatalysis can be defined as the acceleration of a photoreaction in the presence of a catalyst (Ibhadon and Fitzpatrick, 2013). Fujishima and Honda have reported the discovery of photocatalytic splitting of water by a metal oxide photocatalyst called titanium dioxide (TiO_2), under ultraviolet light (UV) (Fujishima and Honda, 1972). Later, Frank and Bard (1977) reported the use of TiO_2 as semiconductor catalyst to decompose cyanide. Ollis and his co-workers (1986) went on further to extensively examine the ability of the heterogeneous photocatalyst to degrade organic molecules. Semiconductors are primary light absorbers widely used as photocatalysts due to their favorable combinations that include the electronic structure, excited-state lifetime, charge transport characteristics, and absorption properties (Thiruvenkatachari et al., 2008).

Furthermore, the currently available water treatment technologies such as adsorption (Foo and Hameed, 2010) or coagulation (Shi et al., 2007) merely concentrate the pollutants present by transferring them to other phase(s) however the pollutants still remain in the system and are not completely eliminated or destroyed (Chong et al., 2010). These spent adsorbents or coagulants later form a secondary waste that require further treatment after the reaction is completed. Since then, more

studies have been done by researchers on photocatalysts, which have prompted numerous and promising TiO₂ applications varying from photocatalysis to photo-electrochromic to sensors (Chen and Mao, 2007; Kim et al., 2010) as well as in biomedicine and cosmetics (Ramelan et al., 2017).

1.4 Titanium dioxide

Titanium dioxide (TiO₂) is a metal oxide semiconductor material which is naturally occur form titanium and is also known as titania. TiO₂ have been widely used in water treatment system because it is cheap, non toxic and readily available. Due to its outstanding electronic properties and chemical stability, photocatalytic reaction using TiO₂ has received huge attention for application as one of the most viable environmental cleanup technologies (Long et al., 2016; Cai et al., 2015).

1.4.1 Properties of titanium dioxide

TiO₂ has been reported to oxidize organic compounds into harmless compounds such as CO₂ and H₂O when irradiated by UV light (Chatterjee and Dasgupta, 2005). Besides, the photocatalytic reaction can take place at room temperature. TiO₂ exists in three major phases which are anatase, rutile, and brookite as shown in **Figure 1.1**. The structure of anatase and rutile is tetragonal, while brookite is an orthorhombic. Among the polymorphs of TiO₂, anatase (band gap energy, 3.2 eV) has been reported to show the best photocatalytic activity compared to other forms of TiO₂ because of its higher electron mobility, lower density, and highly oxidizing and reducing abilities (Lan et al., 2013). Meanwhile, rutile has smaller band gap energy (3.0 eV) and faster electron-hole recombination rate which reduces its efficiency as photocatalyst (Luttrell et al., 2014). Brookite is rarely used because it is difficult to be obtained in pure form without anatase and rutile phases,

therefore its photocatalytic properties has not been much studied (Di Paola et al., 2013).

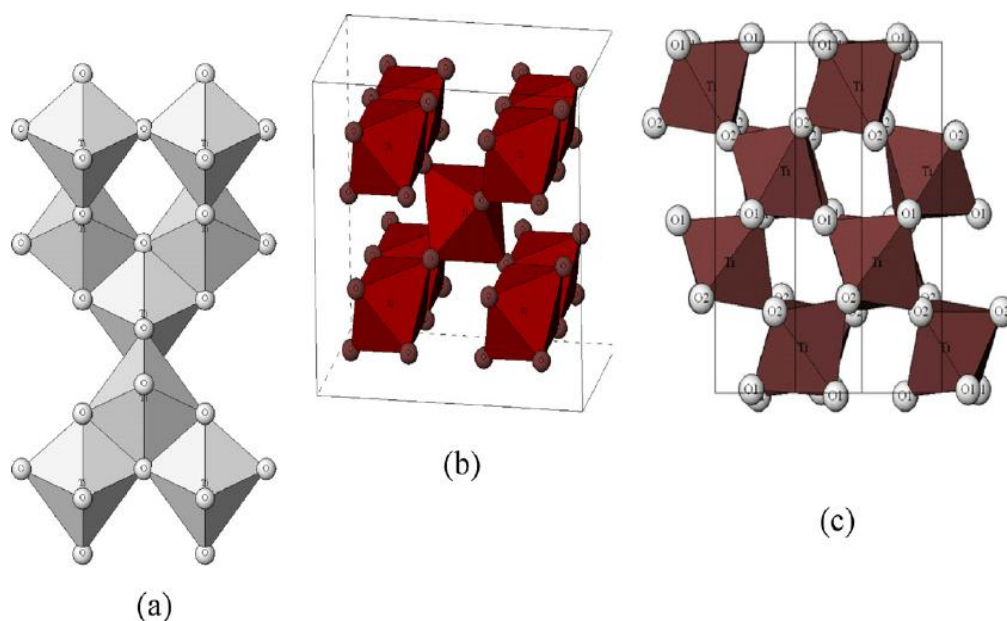


Figure 1.1 Crystalline structures of three different polymorphs of TiO_2 (a) anatase (b) rutile (c) brookite (Pelaez et al., 2012).

TiO_2 is considered as one of the most efficient photocatalyst for the degradation of various organic and inorganic pollutants in water. By the absorption of light energy larger or equal to the band gap of TiO_2 , electrons were excited from the valence band (VB) to conduction band (CB), thus forming electron-hole (e^-/h^+) pairs. These photogenerated charge carriers undergo recombination and become trapped in metastable states or migrate to TiO_2 surface to react with adsorbed molecules (Zaleska, 2008).

In photocatalysis, hydroxyl and superoxide radicals play important roles as active reagents to degrade the pollutants by reacting with the electron-hole pairs. Based on the similar mechanism, TiO_2 can reduce CO_2 to CH_3OH or H_2 under

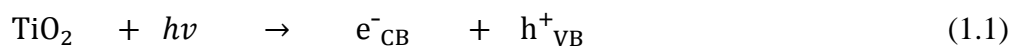
controlled environment such as in inert or oxygen free atmosphere. However, the photocatalytic activity of TiO₂ strongly depends on (Herrmann, 2005):

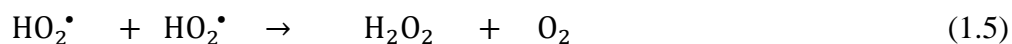
1. Light absorption properties
2. Electron-hole recombinations
3. Reduction and oxidation of semiconductor surface by the e⁻/h⁺ pair

The different properties exhibited by the different TiO₂ polymorph is attributed to the crystal structure of the catalyst. Rutile is thermodynamically the most stable phase, although anatase is formed at lower temperature (< 800 °C). Both of these phases have been known to show photocatalytic activity. Rutile appears to be more suitable for photocatalysis applications because it can absorb light with wider range. However, the anatase phase exhibits superior photocatalytic activity than rutile due to the difference in terms of energy, structure, and the surface area (Herrmann, 2005).

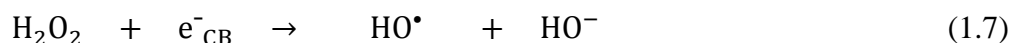
1.4.2 Mechanism of photocatalysis using TiO₂ nanoparticles

TiO₂ is a semiconductive material that acts as a strong oxidizing agent by lowering the activation energy for the decomposition of organic and inorganic substances. The mechanism of the photocatalytic reaction for TiO₂ are shown in the following reactions:





Irradiation by light with energy equals or greater than $h\nu$ produces a hole (h^+) in the valence band, VB and electron (e^-) in the conduction band, CB as shown in Equation 1.1. The hole and electron react with water and oxygen to form hydroxyl radical, HO^\bullet and superoxide radical, $\text{O}_2^{\bullet-}$ as shown in Equations 1.2 to 1.5. The formation of hydrogen peroxide (H_2O_2) will proceed either by undergoing photolysis (Equation 1.6) or by accepting electron (Equation 1.7) to produce hydroxyl radical, HO^\bullet . Hydroxyl radical is a strong oxidizing agent and plays an important role in photocatalysis compared to other oxidizing agents such as O_3 because HO^\bullet reacts 10^6 - 10^{12} times faster to attack organic compounds (Legrini et al., 1993). An adsorbed organic compound, **D**, is a hole trapper therefore it will react with the hole, h^+_{VB} in VB (Equation 1.8).



The TiO_2 photocatalytic reaction requires photo-excitation of light to separate the charge followed by the scavenging of electrons and holes on the surface of the catalyst, **Figure 1.2**.

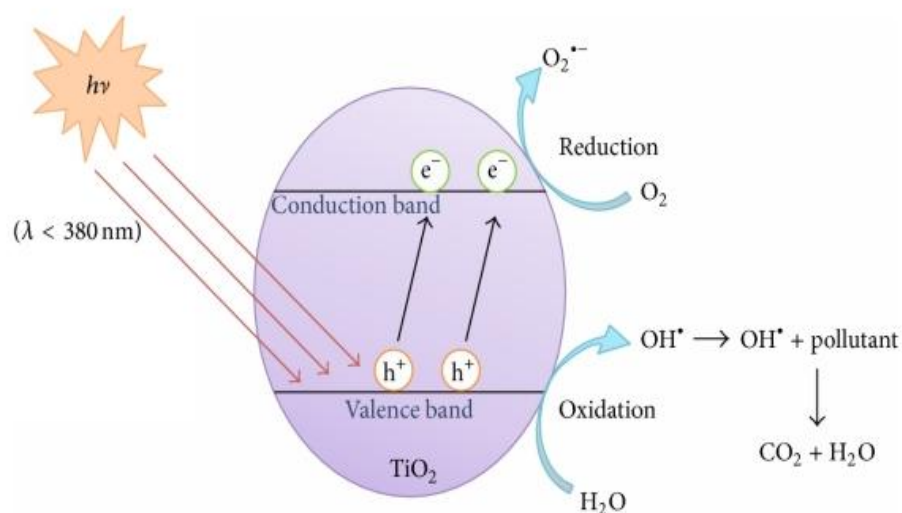


Figure 1.2 Schematic presentation of the mechanism of TiO₂ semiconductor in heterogeneous photocatalysis (Quan et al., 2005).

1.5 Synthesis methods of TiO₂ nanoparticles

There are various methods reported by many researchers to synthesize TiO₂ such as sol-gel (Leong et al., 2014), hydrothermal (Nasir et al., 2014), templating (Zi et al., 2016), and chemical vapor deposition (CVD) (Jais et al., 2016; Rizal et al., 2016). The steps involved during the preparation of the samples are very crucial because it will affect properties such as the crystal structure, the size of the nanoparticles and the morphology of the TiO₂ nanoparticles (Kuwahara et al., 2011).

1.5.1 Sol-gel

The sol-gel method is a versatile process widely used to make ceramic materials and the major benefit of the sol-gel process is the possibility to synthesize pure hybrid organic and inorganic materials (Ciriminna et al., 2013). Sol is a colloidal suspension formed by hydrolysis and polymerization reactions of the precursors, which are usually metal organic compounds or inorganic salts such as metal alkoxides. The complete polymerization and loss of solvent will transform the

liquid sol into a solid gel phase. When the sol is cast into a mold, a wet gel is formed and converted to dense ceramic upon drying and heat treatment. If the solvent in wet gel is removed under a supercritical condition, an aerogel, a highly porous and extremely low-density material is obtained (Pierre, 2002). When the viscosity of sol is adjusted into a proper range, then the ceramic fibers can be drawn from the sol and the nanoparticles is obtained at proper condition (Hench, 1990; Owens, 2016).

Wu and co-workers (2008) have synthesized pure and vanadium (V) doped TiO₂ by sol-gel method and the results showed a red shift in the UV-vis spectra and higher photocatalytic activity under visible light compared to pure TiO₂. On the other hand, Li et al. (2014) developed La³⁺ doped TiO₂ by a sol-gel process and found that La³⁺ doping inhibited the phase transformation of TiO₂, enhancing the thermal stability of the TiO₂ nanoparticles, thus reducing the crystallite size, and increasing the Ti³⁺ content on the surface.

1.5.2 Hydrothermal

The usual hydrothermal method is conducted in a steel pressure vessel known as autoclaves and the reaction took place under controlled temperature and pressure. Hydrothermal and solvothermal method is almost similar as both methods are conducted in autoclaves. However, hydrothermal is highly dependent on the solubility of minerals in hot water because the nutrient is supplied along with water under high pressure (Kharisov et al., 2012). Hydrothermal synthesis has drawn more attention from researchers due to the well crystalline phase formed by using this method. Moreover, the nanoparticles produced have high purity and the desired shape and size of the nanoparticles can be produced by controlling the solute concentration, temperature of the reaction, reaction time and the type of the solvent used (Bae, 2013).

Li et al. (2008) and Bilgin et al. (2015) have synthesized TiO₂ nanoparticles by using this method to degrade MB. Li and his co-workers (2008) synthesized Fe doped TiO₂ via hydrothermal method at 200 °C and this method greatly affected the TiO₂ nanoparticles photocatalytic properties by increasing its activity to degrade MB. Bilgin and his co-workers (2015) also reported that the photocatalytic activity under UV irradiation was increased when TiO₂ nanoparticles prepared by using sol-gel method followed by heating at 130 °C hydrothermally for 36 h.

1.5.3 Templating

The synthesis of nanostructured materials using template method has become extremely popular during the last years (Zhang et al., 2010; Li et al., 2015). In order to construct materials with similar morphology of known characterized materials (templates), this method utilizes the morphological properties of the templates with reactive deposition or dissolution. Therefore, it is possible to prepare numerous new materials with regular or controlled morphology on the nano- and microscale by simply adjusting the morphology of the template material. A variety of templates have been studied for synthesizing titania nanomaterials. For example, Li and his co-workers (2015) have synthesized TiO₂ by using carbon nanotube (CNT) sponge as template while, Zhang et al. (2010) reported that the surface area of TiO₂ was enhanced when mesoporous silica KIT-6 was used as the template. However, the templated method has some disadvantages including the complicated synthetic procedures and in most cases, the templates need to be removed, normally by calcination, leading to an increase in the cost of the materials and the possibility of contamination (Zi et al., 2016).

1.5.4 Chemical vapor deposition (CVD)

Chemical vapor deposition (CVD) is a promising method to synthesize TiO₂ thin films with great quality. CVD is a process where the vapor are condensed to a solid phase material forming thin film. Rizal and co-workers (2016) reported TiO₂ nanoparticles in the form of a thin film on SiO₂/Si prepared via CVD method by using Ti powder as a precursor and O₂ as the carrier gas. The results showed high O₂ flow rates (200 sccm) strongly affected the morphology of TiO₂ nanoparticles and increased the roughness of TiO₂ surface (Rizal et al., 2016). Besides, in the use of TiO₂ thin films deposited onto a glass substrate, parameters such as flow rate, gas composition, deposition pressure and temperature are important in order to obtain TiO₂ nanoparticles with higher photocatalytic activity (Jais et al., 2016; Malekshahi et al., 2013).

1.6 Limitations of TiO₂ nanoparticles

Eventhough TiO₂ have been reported by various authors to show good photocatalytic activity (Malekshahi et al., 2013; Reszczynska et al., 2015), there are still a few limitation of TiO₂ especially in water treatment technology. First, the anatase form of TiO₂ has a wide band gap energy ($E_g \sim 3.2$ eV) therefore higher energy i.e UV light is required to excite electrons to produce hydroxyl radicals for the photodegradation to take place (Leong et al., 2014). Second, the amount of UV light is only about 5 to 8% of the solar spectrum. The UV set-up is expensive and the set up is limited to small scale application for the degradation of organic and inorganic materials in real waste water (Ibhadon and Fitzpatrick, 2013). Apart from that, the electron and hole can recombine easily and this lowers the photocatalytic activity of TiO₂ (Yuanjie et al., 2013). Furthermore, powdered TiO₂ can easily

agglomerate into larger particles and this reduces its efficiency and hinders its practical applications. In addition, the nanosize TiO₂ particles are very small making the separation after the treatment a very difficult process. All these problems restricted the use of TiO₂ for the larger and wider applications. Therefore, in order to overcome these problems, research to improve its photocatalytic activity is gaining much interest from various researchers (Khan et al., 2014; Riaz et al., 2014; Zhu et al., 2012).

1.7 Modification of TiO₂

To improve the properties of TiO₂ nanoparticles, several modifications have been done to increase the photocatalytic activity of TiO₂ semiconductor. The modification can be done by doping TiO₂ with metal or non-metal, dye sensitized, hybrid nanomaterial, and also surface modification by inorganic adsorbent.

1.7.1 Doping with metal

Doping of TiO₂ nanoparticles with transition metals have been reported to narrow the band gap and caused a redshift to the visible light region. This redshift is caused by charge transfer between the d electrons of the transition metals either with the conduction band or the valence band of TiO₂ nanoparticles (Teh and Mohamed, 2011). Pt doped TiO₂ studied by Long et al. (2016) enhanced the photocatalytic activity by degrading 93.4% and 53.6% of MO after 1 h under solar simulator and 80 min under visible light irradiation, respectively. Previously, modification of TiO₂ nanoparticles via Pd doping at different wt % of Pd and different calcination temperatures restrained the anatase to rutile transformation and reduced the TiO₂ grain growth (Cai et al., 2015).

Doping with Fe^{3+} was preferred to be more effective because of its half-filled electronic configuration narrows the band gap and new intermediate energy levels were introduced (Liu et al., 2011). According to Ahmed et al. (2013) doping with Fe^{3+} ion prevented agglomeration and produced well-defined nanocrystalline particles with high surface area thus enhancing the photocatalytic activity by enhancing the adsorption of photons and the degradation of the pollutant. Meanwhile, Giordano and his co-workers (2016) reported Li-doped TiO_2 was able to reduce the (e^-/h^+) recombination rate while other researchers reported Yb^{3+} doped TiO_2 was able to degrade 89% of phenol under visible light after 3 h (Reszczynska et al., 2015).

1.7.2 Doping with non-metal

TiO_2 nanoparticles can also be modified with non-metal elements such as carbon (Kavitha and Devi, 2014), sulfur (Han et al., 2014), or nitrogen (Peng et al., 2008). According to Asahi et al. (2005) the mechanism of non-metal doping is different from the noble and transition metals coupling. For example, N doping introduced new states of the energy level at the valence band edge and caused the original band gap of TiO_2 nanoparticles to become smaller (Wang and Doren, 2005). Modification with N reduced the ratio of rutile to anatase phase thus indicating that N dopants inhibited the transformation of anatase to rutile phase (Iwase et al., 2013). N doping changed the hardness, elastic modulus, electrical conductivity and the refractive index of TiO_2 nanoparticles (Peng et al., 2008). Meanwhile, C doped TiO_2 showed higher photocatalytic activity towards the degradation of 4-chlorophenol (4-CP) under visible light irradiation while the undoped TiO_2 nanoparticles only showed good activity under UV irradiation attributed to wide band gap of undoped TiO_2 .

1.7.3 Hybrid nanomaterials

TiO₂ composites with carbon have been reported to display good results on the photocatalytic activity of TiO₂. Various composites of TiO₂ precursors with carbon materials such as carbon nanotube (CNT) (Reti et al., 2014), graphene (Cheng et al., 2014) and graphene oxide (Stengl et al., 2013) have been reported. TiO₂ multiwalled carbon nanotube (TiO₂/MWCNT) composites have been prepared via hydrolysis of Ti containing precursors adsorbed onto the MWCNT surface followed by annealing at 400 °C to change the amorphous titanium-hydroxide into crystalline nanocatalyst. TiO₂ with 1% wt MWCNT showed excellent degradation of phenol while the 5% wt MWCNT was very efficient for the decomposition of oxalic acid (Reti et al., 2014). Moreover, as carbon acts as photosensitizer by transferring the e⁻ to TiO₂ surfaces, it helps to increase the photocatalytic activity of TiO₂ by extending to the visible light range (Akhavan et al., 2009). Meanwhile, Cheng et al. (2014) prepared graphene film (GF) decorated TiO₂ nano-tube array (GF/TiO₂NTA) electrode by anodization, followed by electrodeposition. The authors stated that graphene in the electrode increased the charge separation and light absorption under both UV and visible lights.

Some of the recent and related studies of TiO₂ nanoparticles prepared based on hybrid nanomaterials and the effect following the modification are summarized in **Table 1.1**.

Table 1.1 Some of the recent studies on hybrid TiO₂ nanomaterial modifications and their effects.

Modifier	Light irradiation condition	Modification effect	References
Carbon nanotube (CNT)	Fluorescent UV lamp (3×40 W); ($\lambda > 365$ nm)	Only anatase phase produced	(Reti et al., 2014)
	Visible light ($\lambda > 420$ nm)	Oxygen vacancies facilitated in TiO ₂	(Chen et al., 2011)
	Ultraviolet light (40 W); ($320 < \lambda < 400$ nm)	Suppressed the recombination of electron-hole pairs	(Li et al., 2014)
Graphene	Xenon lamp (35 W)	Narrow the band gap of anatase to 2.8 eV	(Cheng et al., 2014)
	Xenon lamp (500 W)	High photocatalytic activity	(Zou, 2011)
Graphene oxide (GO)	Fluorescent lamp (13 W); light intensity (3.5 mW cm^2) Narva lamp (emission spectrum > 400 nm)	Hindered electron-hole recombination, exhibited excellent hydrophilic properties	(Stengl et al., 2013)
	365 nm UV light	Photocatalytic activity increased 4 times better than pure TiO ₂	(Dai et al., 2014)
Zinc oxide (ZnO)	365 nm UV light	Recombination rate decreased, enhanced the photocatalytic activity of TiO ₂ enhanced	(Cheng et al., 2014)
	Visible light ($\lambda > 420$ nm); Xenon lamp (500 W)	Enhanced light absorption, Electron transport ability increased, higher degradation efficiency	(Wang et al., 2015)
Tungsten oxide, WO ₃	UV light (15 W Philips UV lamp); Visible light (15 W fluorescent lamp)	Removal efficiency of MB increased	(Jaritkaun, 2016)

1.7.4 Dye sensitization of TiO₂

Recently, dye sensitizers have attracted great attention from researchers as one of the promising clean method to enhance the photocatalytic activity of TiO₂ nanoparticles under visible light irradiation. Dye sensitizer is a method in which the charge generation is done at two places which is at the semiconductor-dye interface and also in the electrolyte (Nazeeruddin et al., 2011). This method has been widely used to degrade pollutants by the incorporation of dye into TiO₂ nanoparticles thus shifting the photocatalytic activity to the visible region. For example, Zyoud et al. (2011) have reported the degradation of methyl orange (MO) under solar simulator radiation by using anthocyanin as the sensitizer. Anthocyanin is a natural molecular dye that is safe to be used and no organic species were traced showing the complete mineralization of the degraded MO.

Recently, Ramelan and his co-workers (2017) reported the efficiency of dye sensitized solar cells (DSSC) increased when anthocyanin from purple sweet potato were used as photosensitizer to fabricate DSSC. Light harvesting efficiency of TiO₂ nanoparticles prepared from sol-gel method was improved by using ZnO as the template for TiO₂ photoanode in dye sensitized solar cells (DSSC) (Pham et al., 2017). Another study reported that the DSSC by N719 dye and sensitized Si/TiO₂ methods enhanced the removal efficiency of N719 dye as Si nanoparticles exhibited luminescent properties and converting the UV ray to the visible ray (Idriss and Ravindra, 2017).

Besides, dye sensitized TiO₂ nanoparticles has received attention in the photovoltaic applications such as in photolysis of water to generate hydrogen (Hirano et al., 2000) and dye sensitized cells (O'Regan and Gratzel, 1991). The efficiency of the dye increased when the position of CB was slightly below the excited state

energy level of various dyes. TiO₂ nanoparticles is the most suitable for this method due to stable photoelectrode in the photoelectrochemical cells which provides the efficiency of the photocatalyst to work well even under extreme conditions.

1.7.5 Modification of TiO₂ by inorganic adsorbates

TiO₂ nanoparticles also can be modified by using inorganic adsorbate such as phosphate. Phosphate modified TiO₂ prepared by phosphoric acid treatment was found to significantly improve the photocatalytic activity under UV irradiation (Zhao et al., 2008). According to the authors, substrates (4-chlorophenol, phenol, and rhodamine B) were removed at higher degradation percentage. This is because the rate of the hydroxyl radicals attack was enhanced since high concentration of phosphate will produce more hydroxyl radicals thus preventing the direct hole oxidation pathway.

Brauer and Szulczewski (2014) have synthesized N doped TiO₂ by sol-gel method and then fluorinated the samples at room temperature. The TiO₂ nanoparticle samples which partially contained anatase phase were tested for the decolorization of MB under visible light and the results showed that the rate of decolorization of MB totally depended on the fluoride concentration as the Ti-OH groups on the TiO₂ surfaces were replaced by Ti-F bonds (Brauer and Szulczewski, 2014).

1.8 Immobilization of TiO₂ nanoparticles

Various materials have been used as supports for TiO₂ nanoparticles in the photodegradation of pollutant in water to reduce the loss of the powdered photocatalyst after treatment, thus many studies have been done to immobilized TiO₂ to overcome this problems. For example, Binaeian et al. (2017) reported TiO₂ immobilized on hexagonal mesoporous silicate loaded with different concentrations

of oak gall tannin to degrade Direct Yellow 86. The analysis showed that TiO₂ nanoparticles immobilized on the tannin loaded mesoporous silicate surface were distributed well without aggregation. In addition, Eddy et al. (2015) have reported that silica improved the photocatalytic activity of TiO₂ nanoparticles by increasing the thermal stability, enhancing the surface area and also providing good sedimentation.

Besides silica, activated carbon (AC) has been shown to improve the photocatalytic activity of TiO₂ nanoparticles (Auta and Hameed, 2011). AC also termed as activated charcoal or activated coal is an amorphous solid carbon derived from carbonaceous source or from plant. AC also shows good synergistic effect by bringing a higher concentration of pollutants in close proximity to the titania active sites and in contact with the hydroxyl radicals for effective photodegradation effect (Sun et al., 2016). Besides, the intermediate formed during degradation will be adsorbed by AC which then undergoes further oxidation (Wang et al., 2009). TiO₂ modified with granular AC (GAC) was used to remove humid acid under UV irradiation (Orha et al., 2016). In photocatalytic degradation, pollutants such as textile dyes were mineralized into nitrate, chloride, and sulfate anions (Mahmoodi et al., 2011).

Polymers such as polyaniline (PANI) and polyvinyl alcohol (PVA) have also been used to immobilize TiO₂ nanoparticles due to their chemical resistance, low density, high durability, and cost effective benefit. For example, Lei et al. (2012) reported that only small amounts of TiO₂ nanoparticles were loss after 25 cycles when TiO₂ were immobilized on PVA. This was attributed to the strong chemical bonds between PVA and TiO₂ which enhanced the potential of the photocatalyst. Meanwhile, PANI has received great interest among researchers because of its high

charge carriers mobility, high absorption in the visible region, cheap, and excellent environmental stability. PANI acted as a support as well as a sensitizer which explained the higher photocatalytic activity compared to TiO₂ nanoparticles alone (Yu et al., 2012).

1.9 Regeneration of TiO₂ nanoparticles

The reusability study of TiO₂ to increase the usage of TiO₂ nanoparticles has gained great concern from various researchers by using H₂O₂ (Gandhi et al., 2012), dielectric barrier discharge (DBD) (Tang et al., 2013), pH solution (Hu and Shipley, 2013) and thermal process (Miranda et al., 2014). For example, Gandhi et al. (2012) reported that TiO₂ nanoparticles can be regenerated by using H₂O₂. The results showed the degradation of phthalic acid remained the same and the values of the rate constants in second and third cycles are almost similar to the fresh catalyst indicating that the activity of the TiO₂ catalyst could be completely restored (Gandhi et al., 2012). However, low amounts of H₂O₂ was reported to cause less hydroxyl radical formation while an excessive amount of H₂O₂ will act as scavange radical (Collivignarelli et al., 2017) which decreased the photocatalytic activity of the nanoparticles.

Dielectric barrier discharge (DBD) is one of the techniques that are able to regenerate of TiO₂. The degradation of phenol increased and can be reused up to four cycles (77%) due to the reaction of TiO₂ with the phenol on the granular Activated Carbon (GAC). This hybrid material is more beneficial because the available active site from TiO₂ and GAC provided higher chances to increase the removal efficiency of phenol (Tang et al., 2013).

Regeneration by photocatalytic oxidation of TiO₂ nanoparticles has also gained attention as one of the techniques to improve the usage of the spent adsorbent. Previously, Liu et al. (2014) reported that zeolite/TiO₂ composite was easily regenerated thus avoiding the production of secondary waste to be treated. The zeolite/TiO₂ synthesized by sol-gel method were tested for the photodegradation for the removal of humic acid and regeneration of the composite. From the photocatalytic oxidation reaction, it was proven that even after five cycles of treatment, there was no significant decrease in the efficiency of zeolite/TiO₂. Moreover, TiO₂ nanoparticles coating on zeolite remains throughout the photocatalysis and the regeneration process (Liu et al., 2014).

Another way to regenerate TiO₂ is by adjusting the pH. Hu and Shipley (2013) reported that even after the 4th cycle, more than 90% of the metals ions (Pb²⁺, Cu²⁺, and Zn²⁺) can be degraded when the pH of the solution was pH 2. Chieng and his co-workers (2015) reported the regeneration efficiency using different eluents followed the trend of NaOH > HNO₃ ≈ H₂O. The regeneration of AC using nitric acid showed similar removal efficiency (between 45 to 43%) for cycles 1 and 2 which was then reduced further to 24% in the 5th cycle. The regeneration by distilled water and nitric acid are almost similar as the removal efficiency decreased from 45 to 20%.

Miranda et al. (2014) compared the regeneration efficiency between thermal process and alkaline treatment (Miranda et al., 2014). The authors have reported thermal process as the best method to regenerate TiO₂ nanoparticles because it was able to degrade most of the contaminants (i.e. caffeine, acetaminophen, ibuprofen and ketorolac).

Shavisi et al. (2014) have studied the removal efficiency of ammonia and reported the regeneration of TiO₂ nanoparticles immobilized on light expanded clay aggregate (TiO₂/LECA) in four steps. Firstly, TiO₂ nanoparticles was washed with water followed by aeration to remove and separate the weak pollutant adsorbed onto the LECA pores. The vital step in this study was when ammonia was removed by soaking the catalyst granules in NaCl solution for 3 h and heating at 250° C. The authors were able to reuse the TiO₂/LECA up to three cycles for the degradation of ammonia in petrochemical wastewater.

1.10 Methylene blue and methyl orange as model pollutants

Methylene blue (MB) and methyl orange (MO), **Figure 1.3**, were used as model pollutants in this study. MB is synthetic basic dye and widely known as a cationic dye. Exposure to MB can lead to health problems such as cyanosis, shock, jaundice and tissue necrosis (Afsaneh et al., 2016).

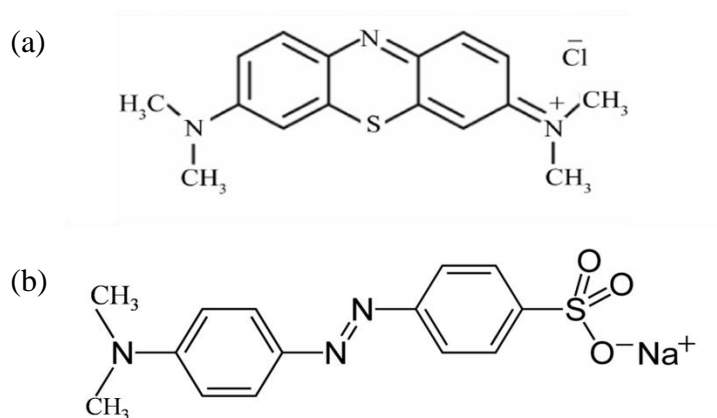


Figure 1.3 The molecular structures of (a) methylene blue (b) methyl orange.

MB is widely used in medicine, pharmaceuticals, analytical chemistry and dye industries (Kumar and Kumaran, 2005; El-Ashtoukhy and Fouad, 2015). Meanwhile, MO is an azo dye and extensively used in textile, leather, paper industries and

sometimes in food preparation (Goh et al., 2010). MO has been reported to cause hypersensitivity, allergy and is known to be highly mutagenic and carcinogenic to human (Trandafilovic et al., 2017). The properties of both MB and MO are summarized in **Table 1.2**.

Table 1.2 Properties of methylene blue and methyl orange (PubChem Compound database)

Properties	Methylene blue	Methyl orange
Appearance	Dark blue	Dark orange
Molecular formula	C ₁₆ H ₁₈ ClN ₃ S	C ₁₄ H ₁₄ N ₃ NaNO ₃ S
Molecular weight (g mol ⁻¹)	319.85	327.33
pKa	3.8	3.4
Solubility in water (g mL ⁻¹)	0.044	0.005
Density (g mL ⁻¹)	0.98	1.28

In the past, most studies related to the removal of MB and MO using TiO₂ nanoparticles was conducted at lower concentrations (5-50 mg/L) (Ahmed et al., 2013; Yang et al., 2015) and as single pollutant (Harikishore, 2014), **Tables 1.3** and **1.4**. In most of the previous reports the concentration of the dye used were low i.e 3 to 50 mg/L, while most of the reported literature used UV light source.

Table 1.3 Summary of the studies on the removal of Methylene blue using TiO₂ in reported literature

Type of dyes	Catalyst	Light Source(s)	Initial dye concentration (mg/L)	Removal efficiency (%)	References
	Ag doped TiO ₂	UV lamp	5	81	Harikishore, 2014
	TiO ₂ /AC	UV lamp (250 W)	25	80	Cifci, 2016
	TiO ₂ /PANI	UV lamp (15 W)	16	70	Ramli et al., 2014
	TiO ₂	UV lamp	33	17	Mainya et al., 2013
	TiO ₂ /AC	UV lamp (15 W)	15	98	Ramli et al., 2014
Methylene blue	Fe ₂ O ₃ /TiO ₂	UV lamp	3	95	Ahmed et al., 2013
	F-TiO ₂	Visible light	25	97	Liu et al., 2017
	TiO ₂ -SiO ₂	Solar lamp (9 W)	50	70	Joseph and Elilarasi, 2017
	Sulfosalicylic acid TiO ₂	UV lamp	15	70	Asadollah and Ali, 2017
	TiO ₂	UV-LED (365 nm)	15	92	Zulmajdi et al., 2017
	CdS/TiO ₂	Xenon lamp (35 W)	10	85	Makama et al., 2016
	PoPD	Xenon lamp (1000 W)	10	90	Yang et al., 2017

Table 1.4 Summary of the studies on the removal of Methyl orange using TiO₂ in reported literature

Type of dyes	Catalyst	Light Source(s)	Initial dye concentration (mg/L)	Removal efficiency (%)	References
	TiO ₂ /ZnO/GO	Xenon lamp (450 W)	50	44	Ramesh et al., 2017
	TiO ₂ /anthocyanin	Lutron LX-102 (0.0212 W/cm ⁻²)	5	95	Zyoud et al., 2011
	TiO ₂	UV lamp	33	20	Mainya et al., 2013
	TiO ₂ (using triboelectric nanogenerator)		20	76	Yuanjie et al., 2013
	Ag doped TiO ₂		15	99	Cifci, 2016
Methyl orange	PVA/TiO ₂	UV lamp (300 nm)	15	73	Lei et al., 2012
	TiO ₂ /CNT	UV lamp (254 nm)	10	80	Park et al., 2013
	Cu doped TiO ₂	UV lamp (350 nm, 250 W)	50	40	Yang et al., 2015
	Si/TiO ₂	UV lamp (4 W)	50	68	Mohammad et al., 2017
	Au/TiO ₂	UV lamp (8 W)	15	100	Silija et al., 2013

1.11 Problem statements

Eventhough, TiO₂ nanoparticles have many advantages for photocatalytic removal of organic and inorganic pollutants, there exist several drawbacks that limit the use of TiO₂ nanoparticles for large scale water treatment technology. The wide band gap of TiO₂ nanoparticles requires UV light irradiation which is expensive, requires special set-up and is limited to small volume of wastewater, while visible light is cheaper and in abundance. In addition to that, the fast e⁻/h⁺ pair recombination rate reduced the photocatalytic activity of TiO₂ nanoparticles. The small nanosized of TiO₂ nanoparticles are easily lost during separation process thus the reusability of the photocatalysis is worth exploring. Most of the existing literature available reported the degradation of single pollutant. In real life, pollutants exist as a mixture and the volume of waste water are very large. Therefore, this study aims to improve the removal efficiency of TiO₂ nanoparticles so that the application can be applied under visible light which is abundant as well as considering binary dye mixture at higher dye concentration, to reflect real industrial effluents which normally exist as a mixture of different types of pollutants.

1.12 Research objectives

- 1) To synthesis a visible light active TiO₂ photocatalyst via Fe doping and immobilization on AC.
- 2) To evaluate the effect of various parameters and compare the degradation and regeneration efficiencies of pure and modified TiO₂ nanoparticles towards single MB, MO, and the binary dye mixture.
- 3) To investigate the reusability of the modified and unmodified TiO₂ materials.